Journal of Molecular Structure 1284 (2023) 135419

Contents lists available at ScienceDirect

Journal of Molecular Structure

journal homepage: www.elsevier.com/locate/molstr

Variable behaviour of a flexible bispyrazole ligand: A Co(II) polymer and a unique Cu(II) penta-coordinated dimer

Joan Soldevila-Sanmartín[a], Teresa Calvet[b], Mercè Font-Bardia[c], Duane Choquesillo-Lazarte[d], Josefina Pons[a,*]

[a] Departament de Química, Universitat Autònoma de Barcelona, 08913 Bellaterra, Barcelona, Spain
[b] Departament de Mineralogia, Petrologia i Geologia Aplicada, Universitat de Barcelona, Martí i Franquès s/n, 08028 Barcelona, Spain
[c] Unitat de Difracció de Raigs-X, Centres Científics i Tecnològics de la Universitat de Barcelona (CCiTUB), Universitat de Barcelona, Solé i Sabarís, 1-3, 08028 Barcelona, Spain
[d] Laboratorio de Estudios Cristalógraficos, IACT (CSIC-Universidad de Granada), Avda. de las Palmeras 4, Armilla, 18100 Granada, Spain

ARTICLE INFO

Article history:
Received 31 January 2023
Revised 20 March 2023
Accepted 23 March 2023
Available online 24 March 2023

Keywords:
Co(II) complexes
Cu(II) complexes
N,O-hybrid ligands
Pyrazole ligands

ABSTRACT

Hoping to highlight the flexibility of a bispyrazole ligand possessing an ether chain including a weak spot (1,2-bis([4-(3,5-*dimethyl*-1*H*-*pyrazol*-1-*yl*)-2-*oxabutyl*]benzene (**L**)), its reactivity against coordinatively flexible metal centres has been assayed. Thus Co(II) and Cu(II) coordination complexes of **L** have been synthesized and fully characterized by analytical and spectroscopical methods. Their X-ray crystal structure elucidation has allowed to ascertain that while the Co(II) compound $\{[Co(\mathbf{L})Cl_2]\cdot 1/2H_2O\}_n$ (**1**) possesses a polymeric structure, much like its Zn(II), Cd(II) and Hg(II) analogues, the Cu(II) compound $[Cu_2\mathbf{L}Cl_4]$ (**2**) displays a completely unexpected dimeric architecture. The previously unreported coordination mode of the ligand in the Cu(II) compound causes dramatical changes in the morphology of the resulting complexes. Their crystal structures are discussed in deep, and the causes behind their differing architectures are examined through comparison with bibliographical references.

1. Introduction

The understanding of the structure-properties relationship in coordination compounds has grown at an astonishing rate during the last decades [1–3]. As such, the development of materials possessing tailored properties through network-based approaches is one of the most researched topics today [1,3–5]. However, the need to develop smarter materials, capable of fulfilling a multi-purpose role, has led to the realization that these demands could be better accomplished by ligands capable of adopting different conformations, and even changing between them as a response to an external stimulus, rather than rigid ones [6–9].

Amongst them, ligands containing *N*-heterocyclic donors linked by flexible chains can adopt surprising conformations owing to the free rotation around the chain, resulting in the formation of coordination compounds bearing unusual architectural motifs or fascinating properties [10–14]. In particular, those with a metalacyclic or polymeric architecture stand out, as they can act as secondary building units for the development of extended frameworks [15,16]. Over the last two decades, our group has been working on the synthesis of such ligands, specializing on those containing pyrazoles as the main functional group. As such, a wide array of polypyrazole ligands bearing amino [17–23], diamino [24–27], thioether [28–32], dithioether [33–37], thiolate [38], sulfone [39,40] and sulfoxide [39] chains have been synthesized, and their reactivity against several metal centres studied. Amongst those mentioned flexible chains, in the last years, those containing alcohol and ether groups have been intensively studied in our group, designing and synthesizing a family of bispyrazole ether ligands [41,42] and testing their reactivity against different metal centres such as Pd(II), Pt(II), Zn(II), Cd(II) and Hg(II) [43–45], resulting in the obtaining of various coordination compounds bearing a wide variety of coordination environments and architectural motifs.

In this sense, we have compared the coordination behaviour of two positional isomers of a bispyrazole ether ligand (Scheme 1): (1,2-bis([4-(3,5-*dimethyl*-1*H*-*pyrazol*-1-*yl*)−2-*oxabutyl*]benzene (*ortho*-isomer) and 1,4-bis([4-(3,5-*dimethyl*-1*H*-*pyrazol*-1-*yl*)−2-*oxabutyl*]benzene (*para*-isomer), against d^{10} metal centers [46], demonstrating that the different orientation of the substituting arms caused a marked preference for the dimeric

* Corresponding author.
E-mail address: josefina.pons@uab.cat (J. Pons).

https://doi.org/10.1016/j.molstruc.2023.135419

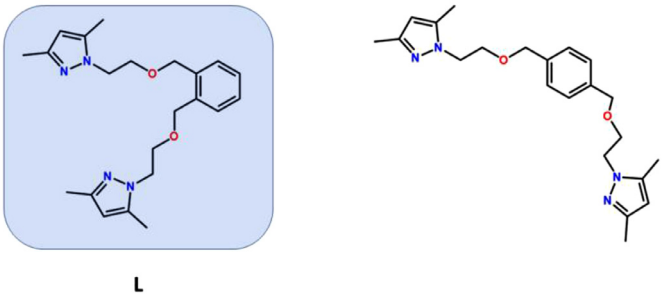

Scheme 1. *Ortho-* (left) and *para-* (right) isomers of a bispyrazole ether ligand. The ligand used in this work is highlighted in blue and labelled.

metalacyclic architecture for the *para-* isomer, while compounds bearing the *ortho-* isomer showed lineal polymeric motifs. Moreover, it was also observed that while the *para-* isomer showed a *NN'*- bridging coordination mode regardless of the metal, the *ortho-*isomer displayed different coordination modes on different metals, such as *NN'*-bridging for Zn(II) and *NON'*-chelating and bridging for Cd(II) and Hg(II) [46].

On this basis, we decided to delve further in the behaviour of the *ortho-* isomer (1,2-bis([4-(3,5-*dimethyl*-1*H*-*pyrazol*-1-*yl*)−2-*oxabutyl*]benzene (**L**)). Our previous studies of the behaviour of **L** against first-row metal cations only included Zn(II) [46]. However, owing to its electronic configuration, the range of available coordination geometries is limited, showing a marked preference for dimeric metallacyclic architectures. Thus, it was decided to expand the study to coordinatively flexible first-row transition metals. Our prior studies similar *N,O*-hybrid pyrazole ligands showed that the use of Cu(II) metal centres afforded a plethora of new arrangements, ranging from mononuclear to tetrameric and even polymeric complexes [47–49] therefore, providing not only variable coordination geometries but also gives access to variable nuclearity. Thus, we hoped that their availability of a wide array of coordination geometries would allow to highlight the ligand's flexibility, resulting in the formation of compounds with previously unreported architectures for **L**. Moreover, the behaviour of this family of compounds against Co(II) has not been reported. Therefore, we first employed Cu(II) to expand our knowledge on this family of *N,O*-hybrid bispyrazole ligands further explored their coordination chemistry with Co(II). Thus, the reactivity of **L** against $MCl_2{\cdot}x(H_2O)$ salt (M = Co(II), $x = 6$; M = Cu(II), $x = 0$) was assayed, resulting in compounds $\{[Co(\mathbf{L})Cl_2]{\cdot}1/2H_2O\}_n$ (**1**) and $[Cu_2(\mathbf{L})Cl_4]$ (**2**).

2. Results and discussion

2.1. Synthesis and general characterization

For the synthesis of these complexes, an ethanolic solution of the corresponding $MCl_2{\cdot}x(H_2O)$ salt (M = Co(II), $x = 6$ (**1**); M = Cu(II), $x = 0$ (**2**)) is added dropwise to an ethanolic solution of 1,2-bis([4-(3,5-*dimethyl*-1*H*-*pyrazol*-1-*yl*)−2-*oxabutyl*]benzene (**L**) in a 1:1 metal to ligand ratio. For **1**, the resulting solution was kept under reflux conditions for 48 h. After that period, the solution was concentrated to a half of its volume and left to evaporate, resulting in the obtaining of a blue precipitate. For **2**, upon then addition of the metal to the ligand solution, a green precipitate appeared immediately. Suitable crystals were obtained by layering a CH_2Cl_2 solution with hexane which was kept in the fridge for one month for **1**, or by recrystallization in EtOH for one month for **2**. Their single crystal X-ray structure revealed that compound **1** is a coordination polymer, $\{[Co(\mathbf{L})Cl_2]{\cdot}1/2H_2O\}_n$, while **2** is a dimeric compound, $[Cu_2(\mathbf{L})Cl_4]$ (Scheme 2).

All compounds were characterized by analytical and spectroscopic techniques. Spectroscopic details of the characterization of all compounds are found in the Exp. Sect. and Supporting Information (S.I.). Recorded powder patterns agree with the elucidated crystal structures (S.I: Figures S1, S2). Elemental analyses (EA) of all compounds agree with the proposed formulae.

The FTIR-ATR spectra of the two compounds in the range of 4000–500 cm^{-1} confirms the coordination of the ligand to the metal centre (S.I. Figures S3, S4). The most characteristic bands of the IR spectra are those corresponding to $[\nu(C = C/C = N)_{ar}]$ (1555–1552 cm^{-1}), $[\delta(C = C/C = N)_{ar}]$ (1440 cm^{-1}), $[\delta(C–H)_{ip}]$ (1103–1058 cm^{-1}) and $[\delta(C–H)_{oop}]$ (840–744 cm^{-1}) [50,51]. These signals are attributable to the pyrazole and phenyl rings present in the ligand. Moreover, for compound **1**, the region between 3600 and 3100 cm^{-1} hosts a broad band attributable to $[\nu(O–H)]$ from H_2O molecules.

The UV–Vis spectra have been recorded in CH_2Cl_2 for **1** and EtOH for **2** ($\approx 1{\cdot}10^{-3}$ M) (S.I: Figures S5, S6). For **1**, the recorded spectrum shows one band in the visible region at 651 nm with a shoulder at 587 nm. These can be attributed to $^4A_2 \rightarrow {}^4T_2$ transitions for Co(II) atoms in a distorted tetrahedral geometry [52–54], which agrees with its elucidated crystal structure. For **2**, the recorded spectrum shows two bands at 678 and a shoulder at 867 nm. For square pyramidal Cu(II) compounds, their recorded UV–Vis spectra may occasionally show a low energy shoulder ($\lambda > 800$ nm) associated to a main broad band between 550 and 700 nm [54,55]. Thus, the signal at 678 nm can be attributed to a $^2E_g \rightarrow {}^2T_{2g}$ transition in a square pyramidal Cu(II) metal centre [56], which is in agreement with its elucidated crystal structure. All ε values (49–361 $M^{-1}cm^{-1}$) are consistent with Laporte-forbidden transitions [56].

2.2. Crystal and extended structure of *1*

Compound **1** crystallizes in the monoclinic crystal system having a C2/c space group, showing a polymeric structure. In it, **L** acts as a bidentate *NN'*-bridged ligand, with an *anti*-conformation (Fig. 1). As stated before, this compound is isostructural with its Zn(II) analogue $\{[Zn(\mathbf{L})Cl_2]{\cdot}1/2H_2O\}_n$ previously reported by our group [46] and shares the polymeric chain motif with $\{[Cd(\mathbf{L})Cl_2]{\cdot}1/2EtOH\}_n$ and $\{[Hg(\mathbf{L})Cl_2]{\cdot}1/2EtOH\}_n$ [46].

Its tetrahedral ($\tau_4 = 0.89$) [57] $[CoN_2Cl_2]$ *core* comprises two chlorine atoms and two nitrogen atoms provided by two differ-

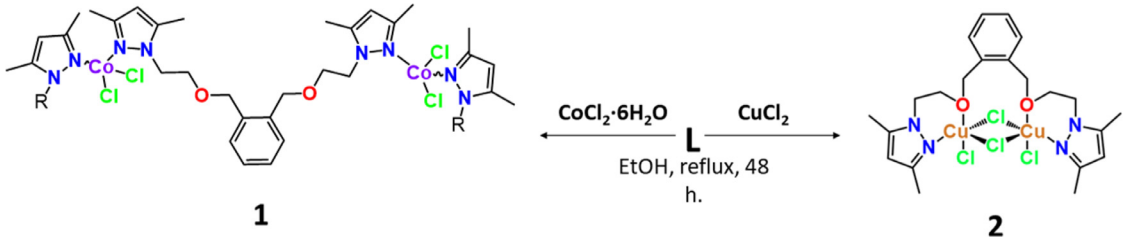

Scheme 2. Synthetic reactions carried out in this work. Compounds are shown with their numbering scheme. Occluded solvent molecules have been removed for clarity.

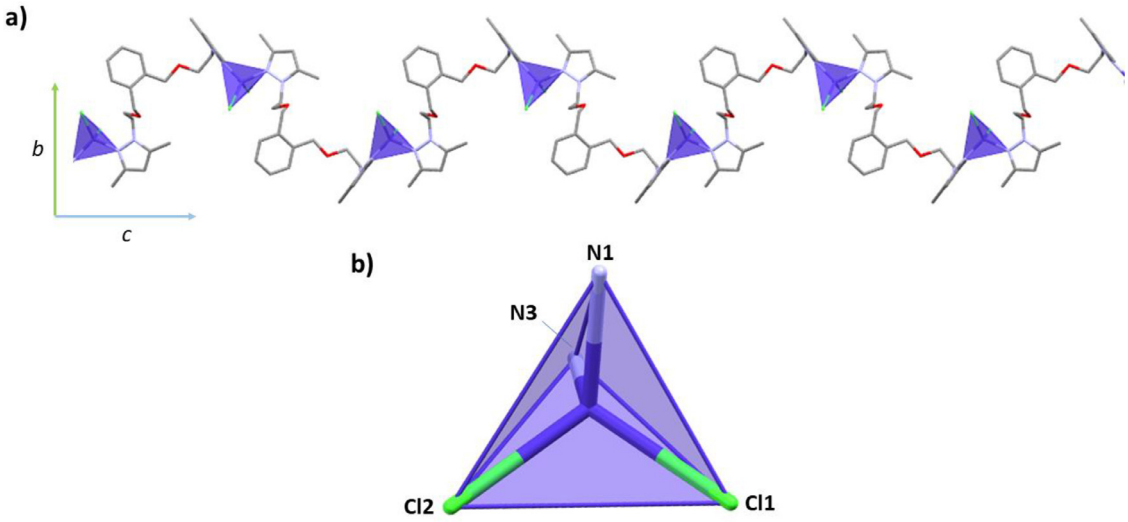

Fig. 1. 1D coordination polymer **1**, showing relevant atoms (a). In detail, the coordination environment around the Co(II) node (b). Solvent molecules (H_2O) and hydrogen atoms have been excluded for clarity.

Table 1
Selected bond lengths (Å), angles (°) and intermolecular interactions of 1.

Bond lengths (Å)				
Co(1)-N(1)	2.0410(16)		Co(1)-Cl(1)	2.2710(6)
Co(1)-N(3)#1	2.0406(17)		Co(1)-Cl(2)	2.2388(6)
Co(1)···Co(1)#1	12.490(9)			
Bond angles (°)				
Cl(1)-Co(1)-Cl(2)	106.79(2)		N(3)#1-Co(1)-Cl(2)	105.53(5)
N(3)#1-Co(1)-Cl(1)	117.54(5)		N(1)-Co(1)-Cl(2)	116.91(5)
N(1)-Co(1)-Cl(1)	106.73(5)		N(1)-Co(1)-N(3)#1	103.86(7)
Intermolecular interactions				
	D-H···A (Å)	D-H (Å)	H-D···A (Å)	>*D*–H···A (°)
O3A-H3A···Cl2	2.572(5)	0.983	3.531(5)	161.41(6)
#1: x, $y + 1$, $z + 1/2$				

ent **L**. A search in the CCDC database [58] reveals the existence of fifty-one reported structures with the same *core*. The vast majority (78.40%) are monomers, while reports of similar compounds bearing polypyrazole bridging ligands are much scarce, with only a handful of dimers (19.64%) [14,59–61] and one polymer (1.96%) [62] being reported.

In **1**, adjacent Co(II) centres are connected by **L** *via* a *NN'*-bidentate bridging mode in an *anti*-conformation, resulting in the formation of an infinite 1D helical chain along the *c* axis (Fig. 1). The distance between repeating units is 23.768(4) Å, while adjacent Co(II) atoms lie at 12.490(9) Å. This distance is larger than those found in related bispyrazole polymer $\{[Co(Me_2bpz)Cl_2]\cdot 1/2H_2O\}_n$ (Me_2bpz = 1,1′-dimethyl-4,4′-bispyrazole) (9.734(2) Å) [62]. The dihedral angle between the mean planes of the pyrazole rings in the centrosymmetric **L** is 68.71(3)°, showing its twisting around the benzene rings. However, alternating pyrazolyl rings, which belong to different **L**, are almost parallel (dihedral angles between mean planes of pyrazolyl rings being 14.5(3)°). Relevant bond lengths and angles for **1** are summarized in Table 1. All values agree with other Co(II) tetrahedral compounds possessing pyrazole and chloride ligands [14,59–62].

The extended structure of this compound is dominated by the presence of occluded H_2O molecules. They bind together a left-handed and a right-handed chain, forming an interesting double supramolecular chain parallel to the crystallographic *c* axis, thanks to a symmetrical double O–H···Cl2 interaction (Fig. 2). The distance between encapsulated water molecules is 13.536(2) Å. They occupy non-connected cavities, which account for 1.8% of unit cell volume (86.91 $Å^3$), calculated defining a prove radius of 1.2 Å (Figure S7). Relevant intermolecular interactions are summarized on Table 1.

2.3. Crystal and extended structure of **2**

Compound **2** crystallizes in the orthorhombic system, having a $Cmc2_1$ space group, showing a dimeric structure (Fig. 3). In it, **L** displays a new coordination behaviour, and a rather unusual one. Moreover, it does not feature a polymeric motif, but a dimeric one. The **L** ligand chelates *via* one nitrogen and one oxygen of each side to a Cu(II) atom, resulting in a *NOO'N'*-chelated and bridged coordination mode in a *syn*-conformation.

In this dimer, Cu(II) atoms adopt a $[CuNOCl_3]$ *core* in a slightly distorted square pyramidal geometry (τ_5 = 0.11) [63]. The basal plane comprises the two bridging chlorine atoms linking two Cu(II) atoms in the same plane, a terminal chlorine atom and one nitrogen atom of the **L** ligand. Finally, the coordination sphere is completed by an oxygen belonging to **L** occupying the apical position, which lies at a longer distance due to Jahn-Teller effect [64].

A search in the CCDC database [58] reveals a total of thirty-one crystal structures bearing a chlorine-bridged dimeric $[CuNOCl_3]$ *core*, but for the immense majority (twenty-nine crystal structures, 93.5%) the apical position is occupied by the bridging chlorine atoms, and only in one case (3.2%) by the oxygen atom [65].

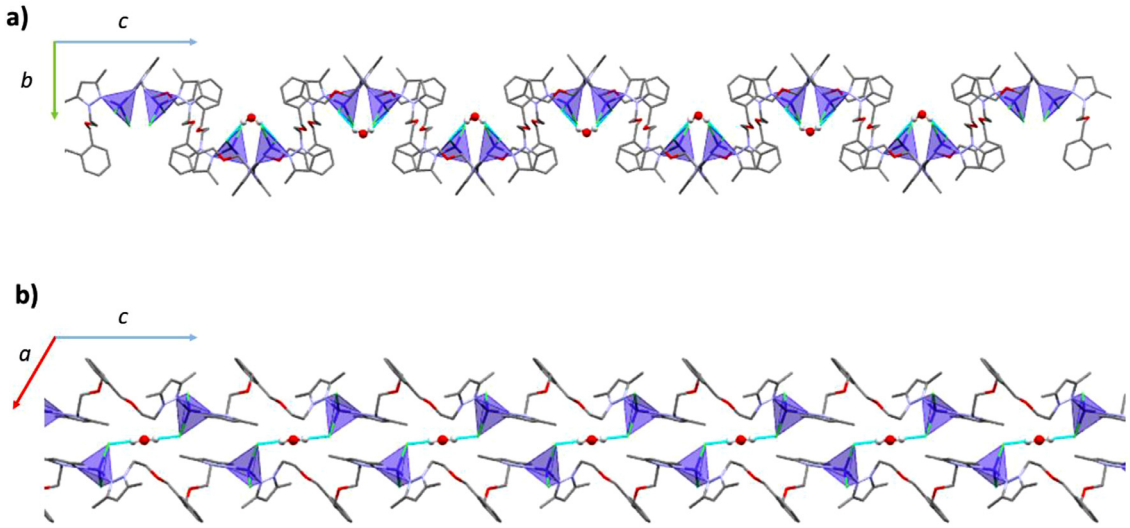

Fig. 2. Supramolecular castellated double chain for polymer **1**, view along a (a) and b (b) axis. Occluded H_2O molecules have been highlighted in the ball and stick mode.

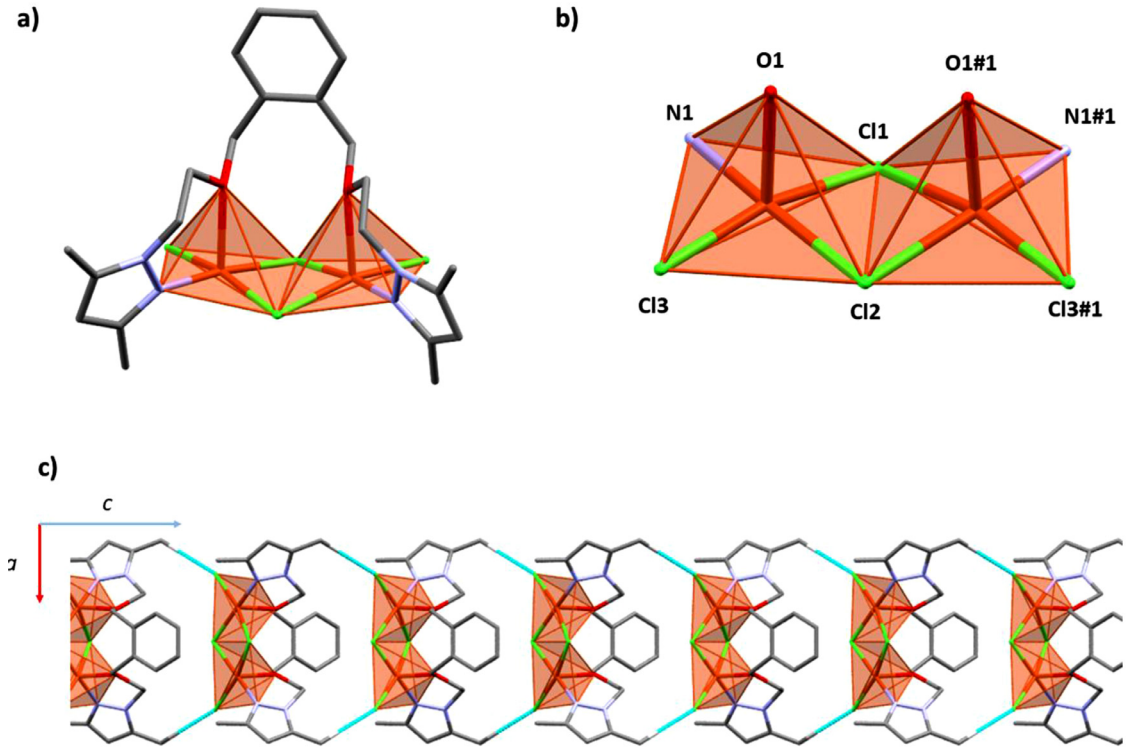

Fig. 3. Compound **2**, showing all its non-hydrogen atoms and their numbering scheme (a). In detail, the coordination environment around the Co(II) node (b). Hydrogen atoms have been excluded for clarity. Supramolecular chain, view along *b* axis (c).

Moreover, of all structures with similar *core*, none of them bears a tetradentate ligand. Due to the spatial constraints induced by the coordination of oxygen atoms. Compound **2** has a peculiar throne shape. In it, the phenyl ring acts as the backrest of the throne, being almost perpendicular (85.7(3)°) to the plane containing the Cu(II) and bridging chlorine atoms. The alkylic chain and the pyrazole groups, which resemble the armrests, bind to the Cu(II) atoms in a *syn-syn* mode, defining planes which intersect at an angle of 70.9(3)° between themselves and at 72.7(3)° with the plane containing the Cu(II) and bridging chlorine atoms. Relevant bond lengths and angles for **2** have been summarized in Table 2. All values agree with related chlorine-bridged dimer [Cu_2(tetra*iso*propylpyridine-2,6-dicarboxamide)$_2Cl_4$] [65].

The supramolecular structure of **2** is dominated by interaction between the terminal chlorine atoms and hydrogen atoms of the alkylic chain. These interactions result in the formation of supramolecular chains along the *c* axis (Fig. 3, Table 2). These chains form a dense network parallel threads arranged in a *zig-zag* pattern.

2.4. Structural discussion

When considering our previously published results of the reactivity of **L** against MCl_2 (M = Zn(II), Cd(II) and Hg(II)) [46], these new results are rather intriguing. While the architectural motif in **1** is similar to those previously reported, compound **2**, possessing

Table 2
Selected bond lengths (Å), angles (°) and intermolecular interactions for 2.

Bond lengths (Å)				
Cu(1)-N(2)	1.977(8)	Cu(1)-Cl(1)	2.321(2)	
Cu(1)-O(1)	2.340(6)	Cu(1)-Cl(2)	2.292(3)	
Cu(1)···Cu(1)	3.348(3)	Cu(1)-Cl(3)	2.292(3)	
Bond angles (°)				
N(1)-Cu(1)-Cl(3)	93.1(3)	N(1)-Cu(1)-O(1)	90.0(3)	
N(1)-Cu(1)-Cl(2)	172.4(3)	Cl(3)-Cu(1)-O(1)	94.28(18)	
Cl(3)-Cu(1)-Cl(2)	92.27(11)	Cl(2)-Cu(1)-O(1)	94.9(2)	
N(1)-Cu(1)-Cl(1)	89.5(3)	Cl(1)-Cu(1)-O(1)	99.93(19)	
Cl(3)-Cu(1)-Cl(1)	165.56(12)	Cu(1)-Cl(1)-Cu(1)#1	92.32(14)	
Cl(2)-Cu(1)-Cl(1)	83.98(11)	Cu(1)#1-Cl(2)-Cu(1)	93.81(14)	
Cl(3)-Cu(1)-Cl(2)	92.27(11)	N(1)-Cu(1)-O(1)	90.0(3)	
Intermolecular interactions				
	D-H···A (Å)	D-H (Å)	H-D···A (Å)	>*D*–H···A (°)
C5-H28···Cl3	2.548(3)	1.089	3.635(3)	176.84(11)
C5-H6···Cl3	2.548(3)	1.089	3.635(3)	176.84(11)
#1: -x, y, z				

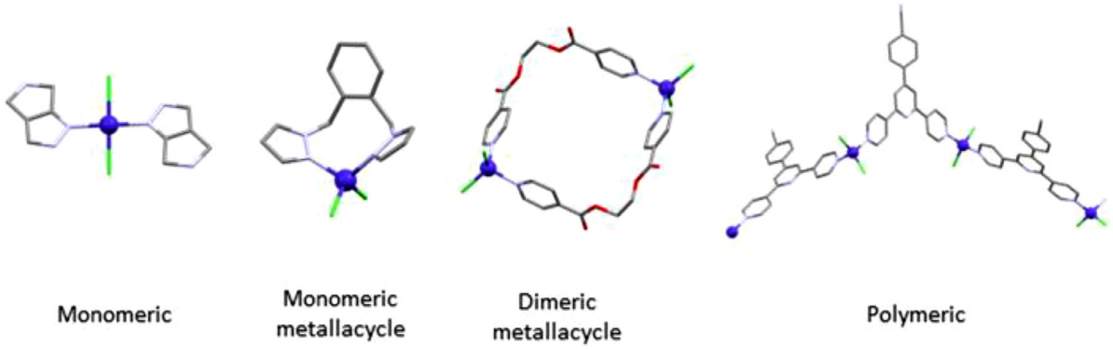

Fig. 4. Most common structural motifs for compounds possessing a $[Co(N_{Pyr})_2Cl_2]$ *core*.

Table 3
Summary of architectural motifs found for CCDC database searches for compounds possessing $[Co(N_{Pz})_2Cl_2]$ and $[Co(N_{Pyr})_2Cl_2]$ *cores*.

	Structural motif	Number (percentage of total)	Examples (CSD REFcode)
$[Co(N_{Pz})_2Cl_2]$	Monomeric	3 (100%)	HEXTEJ [67] HOJHIY [68] HOJHOE [68]
$[Co(N_{Pyr})_2Cl_2]$	Monomeric	61 (80.3%)	ARUFUP [69] DILDUY [70]
	Polymeric	5 (6.6%)	XADBAG [71] DUKWEN [72]
	Dimeric Metallacycle	5 (6.6%)	ASOKOI [73] FILCUA [74]
	Trimeric Metallacycle	2 (2.7%)	JASZEL [75]
	Other	3 (4.0%)	GAQSID [76] OFAYEZ [77]

Cu(II) as metal centre soundly deviates from the expected results, as its architectural motif has not previously been reported for this family of ligands. Thus, we decided to perform a structural study, hoping that it could shed some light on the unusual coordination behaviour of **L** towards Cu(II), when compared to the rest of reported compounds bearing Zn(II), Cd(II), Hg(II) [46] and Co(II).

As stated before, in compound **1, L** shares the same coordination behaviour than in its Zn(II), Cd(II) and Hg(II) compounds, which are all isostructural coordination polymers of general formulae $\{[M(\mathbf{L})Cl_2]\cdot 1/2X\}_n$ (M = Zn(II), X = H_2O; M = Cd(II), Hg(II), X = EtOH) [46], and thus possess the polymeric motif (Fig. 4). However, it is the first time that this motif is reported for compounds bearing a $[Co(N_{Pz})_2Cl_2]$ *core*, as in the only similar structures found in the CCDC database [58], the compound possesses a monomeric metalacyclic or dimeric motif (Fig. 4).

Owing to the scarcity of data (only three reported structures with a $[CoN_{Pz}Cl_2]$ *core* was found in the CCDC database [58]), a similar search was performed for compounds bearing a tetrahedral $[Co(N_{Pyr})_2Cl_2]$ *core* containing the most ubiquitous aromatic *N*-donor, pyridine. Once again, it was found that the overwhelming majority (80.3%, Table 3) of compounds possess the monomeric metalacyclic motif (Fig. 4), while dimeric/trimeric metalacyclic and polymeric motifs are much scarcer (9.4% and 6.6%, respectively, Table 3).

For compound **2**, a search in the CCDC database [58] for similar pyrazole compounds possessing a $[CuN_{Pz}OCl_3]$ *core* surprisingly

Table 4
Summary of architectural motifs found for CCDC database searches for compounds possessing a [Cu(N_{Pyr})OCl_3] *core*.

	Structural motif	Number (percentage of total)	Examples (CSD REFcode)
[Cu(N_{Pyr})OCl_3]	Penta-coordinated dimeric	12 (85.7%)	QUCREO [78] OMOLAF [79]
	Tetrameric	1 (7.1%)	TOGLAC [80]
	Polymeric	1 (7.1%)	TOGLEG01 [81]

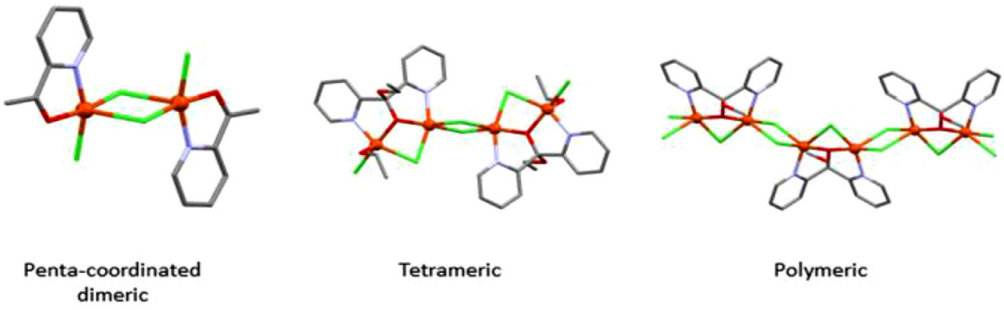

Fig. 5. Most common structural motifs for compounds possessing a [Cu(N_{Pyr})OCl_3] *core*.

retrieves no data, and thus, a search for compounds possessing a [$CuN_{Pyr}OCl_3$] *core*, using the more ubiquitous pyridine ligand instead of a pyrazole ligand, was performed, retrieving fourteen reported structures (Table 4). Most of them (twelve, 85.7%, Table 4) are penta-coordinated Cu(II) dimers, with two bridging chlorine atoms and a third terminal chlorine, much like compound **2**. All of them bear two hybrid *N,O*-donor ligands, while compound **2** would be the first member of this family of compounds to bear only one ligand. The rest of the reported structures bear a tetrameric (one, 7.1%) or a polymeric (1, 7.1%) architectural motif (Table 4, Fig. 5). In any case, for the majority of compound bearing this kind of *core*, the penta-coordinated dimeric motif is the most common one. These data suggests that this motif is highly favoured for Cu(II) metal centres in combination with similar ligands. The energy stabilization deriving from the ligand's chelate effect and the formation of the dimeric *core* may overcome the steric hindrance caused by the *ortho*-substituted arms of the ligand [66], resulting in the obtaining of the penta-coordinated dimeric motif instead of the polymeric one.

3. Conclusions

Two new metal complexes {[Co(L)Cl_2]·1/2H_2O}$_n$ (**1**) and [Cu_2(L)Cl_4] (**2**) containing a flexible bispyrazole ether ligand have been synthesized and fully characterized. Detailed examination of their crystal structures revealed that while compound **1** keeps a polymeric architecture, compound **2** displayed a completely different behaviour, having a penta-coordinated dimeric architecture. This behaviour was rather surprising, as the ligand is expected to adopt an *anti*-conformation (leading to a polymeric architecture) owing to the steric hindrance caused by the *ortho*-substitution of the ligand, instead of the *syn*-conformation adopted in **2**. Moreover, the resulting structure is rather unique, with the ligand adopting a peculiar chair conformation. A thorough search in the CCDC database [55] reveals that for the majority (85.7%) of similar Cu(II) compounds, the penta-coordinated dimeric motif is prevalent, suggesting that it possesses enough stability to overcome the steric hindrance caused by the *ortho*- substitution of the ligands, which favours the polymeric architecture for other metal centres such as Co(II), Zn(II), Cd(II) and Hg(II). Finally, this works highlights the flexibility of **L**, which can adopt several different coordination modes and act as a polytopic ligand through four different coordinative sites.

4. Experimental section

4.1. Materials and general details

Cobalt(II) chloride hexahydrate ($CoCl_2·6H_2O$), copper(II) chloride ($CuCl_2$), ethanol (EtOH), methanol (MeOH) and diethyl ether (Et_2O) were purchased from Sigma Aldrich and used without further purification. Reactions and manipulation were carried out in air at room temperature (r.t.) or reflux conditions. The ligand (**L**) was synthesized according to the procedure reported in the literature [41,43]. Powder X-ray patterns (PXRD) were measured with a Siemens D5000 apparatus (with 40 kW and 45 mA using Cu kα radiation with λ = 1.5406 Å). Patterns were recorded from $2\theta = 5°$ to 40° with a step scan of 0.02° counting for 1 s at each step. Elemental analyses (EA) (C, H, N) were carried out on a Thermo Scientific Flash 2000 CHNS Analyses. FTIR-ATR spectra were recorded on a Tensor 27 (Bruker) spectrometer, equipped with an attenuated total reflectance (ATR) accessory model MKII Golden Gate with diamond window in the range 4000–600 cm^{-1}. The electronic spectra in MeOH ($\approx 1{\cdot}10^{-3}$ M) were run on a JASCO V-780 UV–Visible/NIR Spectrophotometer with a quartz cell having a path length of 1 cm in the range of 500–1100 nm at r.t.

4.2. Synthesis of compound {[Co(L)Cl_2]·1/2H_2O}$_n$ (**1**)

An absolute EtOH (20 mL) solution of $CoCl_2·6H_2O$ (3.18 mmol, 0.754 g) was added dropwise to a solution of **L** (3.18 mmol, 1.22 g) in absolute EtOH (20 mL). The resulting solution was stirred under reflux conditions for 48 h. During this time, the solution shifted from a deep violet colour to a light blue. After that period, the solution was concentrated up to 10 ml and left to evaporate until a blue precipitate appeared. The resulting precipitate was filtered off, washed with 5 mL of cold Et_2O and dried under vacuum.

Suitable crystals for X-ray diffraction were obtained by layering a CH_2Cl_2 solution of the blue precipitate with hexane and leaving it in the fridge at 4 °C for one month.

Yield: 41.8% (0.407 g) Elem Anal. Calc. for $C_{44}H_{62}Cl_4N_8O_5Co_2$ (1042.67): C, 50.68, H 5.99, H 10.75. Found: C 50.75, H 5.78, N 10.43. FTIR-ATR (wavenumber, cm^{-1}): 3370(br) [ν(O–H)], 3135(w)–3078(w) [$\nu(C–H)_{ar}$], 2963(w)–2869(w) [$\nu(C–H)_{al}$], 1552(s) [ν(C = C/C = N)]$_{ar}$, 1466(m), 1440(m) [δ(C = C/C = N)]$_{ar}$, 1420(m), 1371(m), 1352(s), 1311(w), 1263(w), 1218(m), 1186(m), 1124(m), 1100(s), 1094(s) [$\delta(C–H)_{ip}$ + ν(C–O-C)], 1066(s), 1048(s),

876(w), 813(w), 790(s) [δ(C–H)$_{oop}$], 760(vs) [δ(C–H)$_{oop}$], 637(w), 524(w). UV–Vis (MeOH, 1.06·10^{-3} M) λ_{max} (ε(M^{-1}cm^{-1})) = 587 nm (sh, 231), 651 nm (360).

4.3. Synthesis of compound [$Cu_2(L)Cl_4$] (**2**)

An absolute EtOH (20 mL) solution of $CuCl_2$ (3.18 mmol, 0.428 g) was added dropwise to a solution of **L** (3.18 mmol, 1.22 g) in absolute EtOH (20 mL). A green precipitate appeared almost immediately. The resulting solution was stirred at r.t. until no more precipitate appeared. After that period, the resulting green precipitate was filtered off, washed with 5 mL of cold Et_2O and dried under vacuum.

Suitable crystals for X-ray diffraction were obtained *via* recrystallization of the green precipitate in EtOH for one month at r.t.

Yield: 71.6% (0.749 g). Elem. Anal. Calc. for $C_{22}H_{36}Cl_4N_4O_2Cu_2$ (657.40): C 40.19, H 5.52, N 8.52. Found: C 40.30, H 5.47, N 8.35. FTIR-ATR (wavenumber, cm^{-1}): 3132(w)–3089(w) [ν(C–H)$_{ar}$], 2939(w)–2872(w) [ν(C–H)$_{al}$], 1555(s) [ν(C = C/C = N)]$_{ar}$, 1472(m), 1440(m) [δ(C = C/C = N)]$_{ar}$, 1396(m), 1357(w), 1315(s), 1254(m), 1228(w), 1215(w), 1188(w), 1143(w), 1103(s) [ν(C–O-C], 1058(s) [δ(C–H)$_{ip}$], 1014(s), 993(s), 840(s) [δ(C–H)$_{oop}$], 818(m), 785(s) [δ(C–H)$_{oop}$], 744(s) [δ(C–H)$_{oop}$], 635(m), 624(m). UV–Vis (MeOH, 1.25·10^{-3} M) λ_{max} (ε(M^{-1}cm^{-1})) = 678 nm (75), 867 nm (sh, 49).

4.4. X-ray crystallography

For compound **1** data was collected at BL13 (XALOC) [82] at the ALBA synchrotron with an undulator source and channel-cut Si(111) monochromator and Kirkpatrick-Baez focusing mirrors with a selected wavelength of 0.72932. An MD2M-Maatel diffractometer fitted with a Dectris Pilatus 6 M detector was employed. The samples were kept at 100 K with an Oxford Cryosystems 700 series Cryostream. Data was processed with APEX3 suite [83]. The structure was solved by Intrinsic Phasing using the ShelXT program [84], which revealed the position of all non-hydrogen atoms. These atoms were refined on F2 by a full-matrix least- squares procedure using anisotropic displacement parameter [85]. All hydrogen atoms were in difference Fourier maps and included as fixed contributions riding on attached atoms with isotropic thermal displacement parameters 1.2 or 1.5 times those of the respective atom. The OLEX2 software was used as a graphical interface [86].

For compound **2**, a green prism-like specimen was used for the X-ray crystallographic analysis. The X-ray intensity data was measured on a D8 Venture system equipped with a multilayer monochromator and a Mo microfocus (λ = 0.71073 Å). The frames were integrated with the Bruker SAINT software package using a narrow-frame algorithm. Data was corrected for absorption effects using the multi-Scan method (SADABS) [87]. The structure was solved and refined using the Bruker SHELXTL Software Package [84,85]

Crystal data and relevant details of structure refinement are reported in Table 5. Molecular graphics were generated with Mercury 4.1.3 [88,89] with POV-Ray package [90]. Colour codes for molecular graphics: grey (C), white (H), green (Cl), red (O), light blue (N), dark blue (Co), orange (Cu).

Appendix A. Supplementary Data

FTIR-ATR spectra, additional figures and UV–Vis spectra are available as Supporting Information. CCDC 2236407 and 2236667

Table 5
Crystallographic data for compounds **1** and **2**.

	1	2
Empirical Formula	$C_{44}H_{62}Cl_4Co_2N_8O_5$	$C_{22}H_{36}Cl_4Cu_2N_4O_2$
Formula weight	1042.67	657.43
T (K)	100(2)	293(2)
Wavelength (Å)	0.7293	0.71073
System, space group	Monoclinic, C2/c	Orthorhombic, $Cmc2_1$
Unit cell dimensions		
a (Å)	29.9778(10)	21.873(16)
b (Å)	8.0411(3)	7.781(4)
c (Å)	23.7682(8)	15.377(7)
α (°)	90	90
β (°)	122.0530(10)	90
Υ (°)	90	90
V (Å^3)	4856.0(3)	2617(3)
Z	4	4
D_{calc} (mg/m^3)	1.426	1.669
μ (mm^{-1})	1.017	2.062
F (000)	2176	1352
Crystal size (mm^{-3})	0.12 × 0.10 × 0.10	0.068 × 0.062 × 0.043
hkl ranges	$-35 \le h \le 35$, $-9 \le k \le 9$, $-28 \le l \le 28$	$-28 \le h \le 28$, $-10 \le k \le 10$, $-19 \le l \le 19$
θ range (°)	1.841 to 25.722	2.649 to 27.572
Reflections collected/unique /[R_{int}]	33,398 / 4269 / [R_{int}] = 0.0520	15,100 / 3080 / [R_{int}] = 0.2017
Completeness to θ (%)	99.4	99.9
Absorption correction	Semi-empirical	Semi-empirical
Max. and min. transmission	0.0298 and 0.0098	0.7454 and 0.5078
Refinement method	Full-matrix least-square on $\|F\|^2$	Full-matrix least-square on $\|F\|^2$
Data/Restrains/Parameters	4269 / 0 / 289	3080 / 1 / 159
Goodness-on-fit on $\|F\|^2$	1.039	1.029
Final R indices [$I>2\sigma$(I)]	R1= 0.0379 wR2= 0.1115	R1= 0.0607 wR2= 0.0997
R indices (all data)	R1= 0.0382 wR2= 0.1118	R1= 0.1282 wR2= 0.1196
Extinction coefficient	n/a	n/a
Largest diff. peak and hole (e.Å^{-3})	0.568 and −0.457	0.805 and −0.679

contain the supplementary crystallographic data for this paper. These data can be obtained free of charge via http://www.ccdc.cam.ac.uk/conts/retrieving.html or from the Cambridge Crystallographic centre, 12 Union Road, Cambridge CB2 1 Ez, UK; fax: (+44)1223–336–033; or e-mail: deposit@ccdc.cam.ac.uk.

Declaration of Competing Interest

The authors declare that they have no known competing financial interests or personal relationships that could have appeared to influence the work reported in this paper.

CRediT authorship contribution statement

Joan Soldevila-Sanmartín: Investigation, Visualization, Writing – original draft. **Teresa Calvet:** Validation, Resources, Funding acquisition, Writing – review & editing. **Mercè Font-Bardia:** Validation, Formal analysis, Data curation. **Duane Choquesillo-Lazarte:** Validation, Formal analysis, Data curation. **Josefina Pons:** Conceptualization, Validation, Resources, Writing – review & editing, Supervision, Project administration, Funding acquisition.

Data availability

Data will be made available on request.

Acknowledgements

J.P. thanks CB615921 project, the CB616406 project from "Fundació La Caixa" and the Generalitat de Catalunya (2017/SGR/1687). J.S. also acknowledges the PIF pre-doctoral Fellowship from the Universitat Autònoma de Barcelona for his pre-doctoral grant. Some of the experiments were performed at the XALOC beamline of the ALBA synchrotron with support of the ALBA staff.

Supplementary materials

Supplementary material associated with this article can be found, in the online version, at doi:10.1016/j.molstruc.2023.135419.

References

[1] W. Lu, Z. Wei, Z.Y. Gu, T.F. Liu, J. Park, J. Park, J. Tian, M. Zhang, Q. Zhang, T. Gentle, M. Bosch, H.C. Zhou, Tuning the structure and function of metal-organic frameworks via linker design, Chem. Soc. Rev. 43 (2014) 5561–5593, doi:10.1039/c4cs00003j.

[2] J. Luo, J.-W. Wang, J.-H. Zhang, S. Lai, D.-C. Zhong, Hydrogen-bonded organic frameworks: design, structures and potential applications, CrystEngComm 20 (2018) 5884–5898, doi:10.1039/C8CE00655E.

[3] G. Maurin, C. Serre, A. Cooper, G. Férey, The new age of MOFs and of their porous-related solids, Chem. Soc. Rev. 46 (2017) 3104–3107, doi:10.1039/C7CS90049J.

[4] P. Silva, S.M.F. Vilela, J.P.C. Tomé, F.A. Almeida Paz, Multifunctional metal–organic frameworks: from academia to industrial applications, Chem. Soc. Rev. 44 (2015) 6774–6803, doi:10.1039/C5CS00307E.

[5] Z. Zhang, M.J. Zaworotko, Template-directed synthesis of metal–organic materials, Chem. Soc. Rev. 43 (2014) 5444–5455, doi:10.1039/C4CS00075G.

[6] T.F. Liu, J. Lü, R. Cao, Coordination polymers based on flexible ditopic carboxylate or nitrogen-donor ligands, CrystEngComm 12 (2010) 660–670, doi:10.1039/b914145f.

[7] R.E. Morris, L. Brammer, Coordination change, lability and hemilability in metal–organic frameworks, Chem. Soc. Rev. 46 (2017) 5444–5462, doi:10.1039/C7CS00187H.

[8] F. Tan, A. López-Periago, M.E. Light, J. Cirera, E. Ruiz, A. Borrás, F. Teixidor, C. Viñas, C. Domingo, J.G. Planas, An unprecedented stimuli-controlled single-crystal reversible phase transition of a metal–organic framework and its application to a novel method of guest encapsulation, Adv. Mater. 30 (2018) 1800726, doi:10.1002/adma.201800726.

[9] C.J. Sumby, Bridging ligands comprising two or more di-2-pyridylmethyl or amine arms: alternatives to 2,2'-bipyridyl-containing bridging ligands, Coord. Chem. Rev. 255 (2011) 1937–1967, doi:10.1016/j.ccr.2011.03.015.

[10] I. Bassanetti, C. Atzeri, D.A. Tinonin, L. Marchiò, Silver(I) and thioether-bis(pyrazolyl)methane ligands: the correlation between ligand functionalization and coordination polymer architecture, Cryst. Growth Des. 16 (2016) 3543–3552, doi:10.1021/acs.cgd.6b00506.

[11] D.L. Reger, A.E. Pascui, M.D. Smith, J. Jezierska, A. Ozarowski, Syntheses, structural, magnetic, and electron paramagnetic resonance studies of mono-bridged cyanide and azide dinuclear copper(ii) complexes: antiferromagnetic superexchange interactions, Inorg. Chem. 54 (2015) 1487–1500, doi:10.1021/ic502485p.

[12] D.L. Reger, A.E. Pascui, E.A. Foley, M.D. Smith, J. Jezierska, A. Ozarowski, Dinuclear metallacycles with single M-O(H)-M bridges [M = Fe(II), Co(II), Ni(II), Cu(II)]: effects of large bridging angles on structure and antiferromagnetic superexchange interactions, Inorg. Chem. 53 (2014) 1975–1988, doi:10.1021/ic4017905.

[13] A. Beheshti, A. Lalegani, G. Bruno, H. Amiri Rudbari, Investigating the effect of flexible ligands on the crystal engineering of the iron(II) coordination compounds, J. Mol. Struct. 1051 (2013) 244–249, doi:10.1016/j.molstruc.2013.08.023.

[14] D.L. Reger, A.E. Pascui, E.A. Foley, M.D. Smith, J. Jezierska, A. Wojciechowska, S.A. Stoian, A. Ozarowski, Dinuclear metallacycles with single M–X–M bridges (X = Cl –, Br – ; M = Fe(II), Co(II), Ni(II), Cu(II), Zn(II), Cd(II)): strong antiferromagnetic superexchange interactions, Inorg. Chem. 56 (2017) 2884–2901, doi:10.1021/acs.inorgchem.6b02933.

[15] U.P. Singh, N. Singh, S. Chandra, Construction and structural diversity of Cd-MOFs with pyrazole based flexible ligands and positional isomer of naphthalenedisulfonate, Inorg. Chem. Commun. 61 (2015) 35–40, doi:10.1016/j.inoche.2015.08.009.

[16] C.S. Hawes, B. Moubaraki, K.S. Murray, P.E. Kruger, D.R. Turner, S.R. Batten, Exploiting the pyrazole-carboxylate mixed ligand system in the crystal engineering of coordination polymers, Cryst. Growth Des. 14 (2014) 5749–5760, doi:10.1021/cg501004u.

[17] J. Pons, J. García-Antón, M. Font-Bardia, T. Calvet, J. Ros, Coordination compounds of Cd(II) with several bidentate-NN′ and tridentate-NN′N nitrogen donor ligands. 113Cd NMR studies of monomeric compounds containing nitrogen donor atoms, Inorganica Chim. Acta. 362 (2009) 2698–2703, doi:10.1016/j.ica.2008.12.009.

[18] M. del Carme Castellano, J. Pons, J. García-Antón, X. Solans, M. Font-Bardia, J. Ros, Synthesis of new platinum(II) compounds with several bidentate and tridentate nitrogen-donor ligands. Structural analyses by 1H, 13C{1H} and 195Pt{1H} NMR spectroscopy and X-ray crystal structure, Inorganica Chim. Acta. 361 (2008) 2491–2498, doi:10.1016/j.ica.2008.01.016.

[19] M. del C. Castellano, J. Pons, J. García-Antón, X. Solans, M. Font-Bardía, J. Ros, Coordination compounds of Zn(II) with several bidentate-NN′ and tridentate-NN′N nitrogen donor ligands, Inorganica Chim. Acta. 361 (2008) 2923–2928, doi:10.1016/j.ica.2008.02.059.

[20] G. Esquius, J. Pons, R. Yáñez, J. Ros, Organometallic rhodium (I) complexes with 1-alkylaminopyrazole ligands, J. Organomet. Chem. 619 (2001) 14–23, doi:10.1016/S0022-328X(00)00662-8.

[21] R. Mathieu, G. Esquius, N. Lugan, J. Pons, J. Ros, Bis[(3,5-*dimethyl*-1-*pyrazolyl*)*methyl*]ethylamine – a versatile ligand for complexation in RhI cationic complexes, Eur. J. Inorg. Chem. (2001) 2683–2688 2001, doi:10.1002/1099-0682(200109)2001:10⟨2683::AID-EJIC2683⟩3.0.CO;2-T.

[22] A. Pañella, J. Pons, J. García-Antón, X. Solans, M. Font-Bardia, J. Ros, Exploring the coordination chemistry and reactivity of hemilabile N-alkylaminopyrazole ligands towards Pd(II), Inorganica Chim. Acta. 359 (2006) 4477–4482, doi:10.1016/j.ica.2006.05.046.

[23] G. Aragay, J. Pons, J. García-Antón, Á. Mendoza, G. Mendoza-Díaz, T. Calvet, M. Font-Bardia, J. Ros, Synthesis and characterization of new palladium(II) complexes containing N-alkylamino-3,5-diphenylpyrazole ligands. Crystal structure of [PdCl(L2)](BF4) {L2 = Bis[2-(3,5-*diphenyl*-1-*pyrazolyl*)*ethyl*]ethylamine}, Aust. J. Chem. 62 (2009) 475, doi:10.1071/CH08521.

[24] G. Zamora, J. Pons, J. Ros, Rh(I) complexes containing tris(pyrazolyl)amine and bis(pyrazolyl)amine ligands: synthesis and NMR studies, Inorganica Chim. Acta. 357 (2004) 2899–2904, doi:10.1016/j.ica.2004.02.037.

[25] G. Zamora, J. Pons, X. Solans, M. Font-Bardia, J. Ros, Study of the reactivity of tris(pyrazolyl)amine and bis(pyrazolyl)amine ligands toward Rh(I). Crystal structure of [Rh3Cl3(cod)3tdma]·CH3CN (tdma=tris[(3,5-*dimethyl*-1-*pyrazolyl*)*methyl*]amine), a C3-symmetric compound, J. Organomet. Chem. 689 (2004) 980–986, doi:10.1016/j.jorganchem.2003.12.036.

[26] M. Espinal, J. Pons, J. García-Antón, X. Solans, M. Font-Bardia, J. Ros, Synthesis of new palladium(II) complexes containing tetradentate-nitrogen donor ligands: combined structural studies by NMR spectroscopy and X-ray crystallography, Inorganica Chim. Acta. 361 (2008) 2648–2658, doi:10.1016/j.ica.2007.11.011.

[27] M. Espinal, J. Pons, J. García-antón, X. Solans, M. Font-bardia, J. Ros, Unexpected formation of [Pd(bedp)][Pd2Cl4(μ-SMe)2] (bedp = 1,4-bis[2-(3,5-*dimethyl*-1-*pyrazolyl*)*ethyl*]piperazine). Structural characterisation and spectroscopic properties, Inorg. Chem. Commun. 12 (2009) 368–370, doi:10.1016/j.inoche.2009.02.016.

[28] J. García-Antón, J. Pons, X. Solans, M. Font-Bardia, J. Ros, Synthesis of new PdII complexes containing a thioether-pyrazole hemilabile ligand– structural analysis by1H,13C NMR spectroscopy and crystal structure of [PdCl(bdtp)]BF4 [bdtp = 1,5-Bis(3,5-dimethyl-1-pyrazolyl)-3-thiapentane], Eur. J. Inorg. Chem. (2003) 3952–3957 2003, doi:10.1002/ejic.200300235.

[29] A. de León, J. Pons, J. García-Antón, X. Solans, M. Font-Bardía, J. Ros, Reactivity of [PdCl(bdtp)](BF4) with monodentate neutral and anionic ligands. Structure of [Pd(bdtp)(PPh3)](BF4)2 (bdtp=1,5-bis(3,5-dimethyl-1-pyrazolyl)-3-thiapentane), Inorganica Chim. Acta 362 (2009) 3801–3806, doi:10.1016/j.ica.2009.04.045.

[30] A. De León, J. Pons, J. García-Antón, J. Ros, Reactivity of [PdCl2(bdtp)] (bdtp=1,5-bis(3,5-dimethyl-1-pyrazolyl)-3-thiapentane) with neutral and anionic ligands, Polyhedron 29 (2010) 2318–2323, doi:10.1016/j.poly.2010.04.033.

[31] A. de León, J. Antonio Ayllón, J. Pons, Tuning the hemilabile behaviour of a thioether–pyrazole ligand on Pd(II) complexes with diphosphines, J. Organomet. Chem. 696 (2012) 4275–4280, doi:10.1016/j.jorganchem.2011.10.003.

[32] A. de Leon, J. Pons, J. García-Antón, X. Solans, M. Font-Bardia, J. Ros, New Pt(II) complexes containing hemilabile thioether-pyrazole ligands. Structural analysis by 1H, 13C{1H} and 195Pt{1H} NMR spectroscopy and crystal structure of [PtCl(bdtp)](BPh4) [bdtp=1,5-bis(3,5-dimethyl-1-pyrazolyl)-3-thiapentane], Polyhedron 26 (2007) 2498–2506, doi:10.1016/j.poly.2006.12.034.

[33] J. García-Antón, J. Pons, X. Solans, M. Font-Bardia, J. Ros, Synthesis of new PdII complexes containing thioether−pyrazole hemilabile ligands − structural analysis by 1H and 13C NMR spectroscopy and crystal structures of [PdCl2(bddo)] and [Pd(bddo)](BF4)2 [bddo = 1,8-Bis(3,5-dimethyl-1-pyrazolyl)-3,6-dithiaoctane], Eur. J. Inorg. Chem. (2002) 3319–3327 2002, doi:10.1002/1099-0682(200212)2002:12⟨3319::AID-EJIC3319⟩3.0.CO;2-L.

[34] J. García-Antón, J. Pons, J. Ros, X. Solans, M. Font-Bardia, [1,9-Bis(3,5-dimethylpyrazol-1-yl-κ N 2)-3,7-dithianonane-κ 2 S,S ′]palladium(II) bis(tetrafluoroborate), Acta Crystallogr. Sect. E Struct. Reports Online. 60 (2004) m1087–m1089, doi:10.1107/S1600536804016022.

[35] A. de Leon, J. Pons, J. García-Antón, X. Solans, M. Font-Bardia, J. Ros, Synthesis, Structural Characterization and Spectroscopic Properties of [Pt(bddn)]Cl2 · 3·5H2O (bddn = 1,9-bis(3,5-dimethyl-1-pyrazolyl)-3,7-dithianonane), J. Chem. Crystallogr. 37 (2007) 801–805, doi:10.1007/s10870-007-9251-4.

[36] A. de León, J. Pons, J. García-Antón, X. Solans, M. Font-Bardía, J. Ros, Preparation and characterisation of mononuclear Pd(II) complexes with 1,8-bis(3,5-dimethyl-1-pyrazolyl)-3,6-dithiaoctane (bddo) ligand: spectroscopy studies and crystal structure of trans-[*Pd*(SCN)2(*bddo*)], Polyhedron 28 (2009) 2165–2170, doi:10.1016/j.poly.2009.04.013.

[37] A. de Leon, J. Pons, J. García-Antón, X. Solans, M. Font-Bardia, J. Ros, Synthesis of new platinum(II) complexes containing hybrid thioether–pyrazole ligands: structural analysis by 1H and 13C{1H} NMR spectroscopy and X-ray crystal structures, Inorganica Chim. Acta. 360 (2007) 2071–2082, doi:10.1016/j.ica.2006.10.035.

[38] J. García-Antón, J. Pons, X. Solans, M. Font-Bardia, J. Ros, Synthesis, X-ray crystal structure, and NMR characterisation of thiolate-bridged dinuclear Ni(II), Pd(II) and Pt(II) complexes of didentate ligands with NS-donor set, Inorganica Chim. Acta. 355 (2003) 87–94, doi:10.1016/S0020-1693(03)00333-5.

[39] A. de León, J. García-Antón, J. Ros, G. Guirado, I. Gallardo, J. Pons, Environmentally benign and selective synthesis of hybrid pyrazole sulfoxide and sulfone ligands, New J. Chem. 37 (2013) 1889, doi:10.1039/c3nj00161j.

[40] A. De León, M. Guerrero, J. García-Antón, J. Ros, M. Font-Bardía, J. Pons, Study of new metallomacrocyclic Pd(II) complexes based on hybrid pyrazole sulfoxide/sulfone ligands and their contribution to supramolecular networks, CrystEngComm 15 (2013) 1762–1771, doi:10.1039/c2ce26687c.

[41] M. Guerrero, J. Garciá-Antón, M. Tristany, J. Pons, J. Ros, K. Philippot, P. Lecante, B. Chaudret, Design of new N,O hybrid pyrazole derived ligands and their use as stabilizers for the synthesis of Pd nanoparticles, Langmuir 26 (2010) 15532–15540, doi:10.1021/la1016802.

[42] M. Guerrero, J. Pons, M. Font-Bardia, T. Calvet, J. Ros, Synthesis, structural characterization and spectroscopic properties of 1,2-bis[4-(3,5-*dimethyl*-1H-*pyrazol*-1-*yl*)-2-*oxobutyl*]benzene, J. Chem. Crystallogr. 41 (2011) 721–726, doi:10.1007/s10870-010-9960-y.

[43] M. Guerrero, J. Pons, V. Branchadell, T. Parella, X. Solans, M. Font-Bardia, J. Ros, Synthesis and characterization of metallomacrocyclic palladium(II) complexes with new hybrid pyrazole ligands. Diffusion NMR studies and theoretical calculations, Inorg. Chem. 47 (2008) 11084–11094, doi:10.1021/ic8013915.

[44] M. Guerrero, J. Pons, T. Parella, M. Font-Bardia, T. Calvet, J. Ros, Variable coordination behavior of new hybrid pyrazole ligand: synthesis and characterization of several Zn II, Cd II, Hg II, Pd II, Pt II, and Ni II complexes, Inorg. Chem. 48 (2009) 8736–8750, doi:10.1021/ic900908n.

[45] M. Guerrero, J. Pons, J. Ros, M. Font-Bardia, V. Branchadell, Anion influence on the structure of N,O -hybrid pyrazole Zn II, Cd II, and Hg II complexes. Synthesis, characterization, and theoretical studies, Cryst. Growth Des. 12 (2012) 3700–3708, doi:10.1021/cg300506c.

[46] J. Soldevila-Sanmartín, M. Guerrero, D. Choquesillo-Lazarte, J. Giner Planas, J. Pons, Dimeric metallacycles and coordination polymers: Zn(II), Cd(II) and Hg(II) complexes of two positional isomers of a flexible N,O-hybrid bispyrazole derived ligand, Inorganica Chim. Acta 506 (2020) 119549, doi:10.1016/j.ica.2020.119549.

[47] A.M. López Marzo, M. Guerrero, T. Calvet, M. Font-Bardia, E. Pellicer, M.D. Baró, J. Pons, J. Sort, New binuclear copper(II) coordination polymer based on mixed pyrazolic and oxalate ligands: structural characterization and mechanical properties, RSC Adv. 5 (2015) 32369–32375, doi:10.1039/C5RA04028K.

[48] M. Guerrero, T. Calvet, M. Font-Bardia, J. Pons, Synthesis and characterization of Pd(II), Pt(II), Cu(I), Ag(I) and Cu(II) complexes with N,O-hybrid pyrazole ligand, Polyhedron 119 (2016) 555–562, doi:10.1016/j.poly.2016.09.004.

[49] J. Soldevila-Sanmartín, T. Calvet, M. Font-Bardia, J.G. Planas, J. Pons, Copper complexes from 3,5-disubstituted N-hydroxyethylpyrazole ligands: cleavage of C N bond as well as formation of second coordination sphere complexes, Polyhedron 211 (2022) 115543, doi:10.1016/j.poly.2021.115543.

[50] K. Nakamoto, Infrared and Raman spectra of inorganic and, Handb, Vib. Spectrosc. (2006) 1872–1892, doi:10.1002/9780470027325.s4104.

[51] K. Nakamoto, Infrared and Raman Spectra of Inorganic and Coordination Compounds, 1st ed., John Wiley & Sons, Inc., Hoboken, NJ, USA, 2008, doi:10.1002/9780470405840.

[52] S.S. Massoud, L.Le Quan, K. Gatterer, J.H. Albering, R.C. Fischer, F.A. Mautner, Structural characterization of five-coordinate copper(II), nickel(II), and cobalt(II) thiocyanato complexes derived from bis(2-(3,5-dimethyl-1-pyrazolyl)ethyl)amine, Polyhedron 31 (2012) 601–606, doi:10.1016/j.poly.2011.10.011.

[53] S.S. Kandil, G.B. El-Hefnawy, E.A. Baker, Thermal and spectral studies of 5-(phenylazo)-2-thiohydantoin and 5-(2- hydroxyphenylazo)-2-thiohydantoin complexes of cobalt(II), nickel(II) and copper(II), Thermochim. Acta. 414 (2004) 105–113, doi:10.1016/j.tca.2003.11.021.

[54] S.S. Massoud, F.R. Louka, Y.K. Obaid, R. Vicente, J. Ribas, R.C. Fischer, F.A. Mautner, Metal ions directing the geometry and nuclearity of azido-metal(ii) complexes derived from bis(2-(3,5-dimethyl-1H-pyrazol-1-yl)ethyl)amine, Dalt. Trans. 42 (2013) 3968, doi:10.1039/c2dt32540c.

[55] S.S. Massoud, M. Spell, C.C. Ledet, T. Junk, R. Herchel, R.C. Fischer, Z. Trávníček, F.A. Mautner, Magnetic and structural properties of dinuclear singly bridged-phenoxido metal(⟨scp⟩ii⟨/scp⟩) complexes, Dalt. Trans. 44 (2015) 2110–2121, doi:10.1039/C4DT03508A.

[56] B.J. Hathaway, Copper, Coord. Chem. Rev. 35 (1981) 211–252, doi:10.1016/S0010-8545(00)80463-4.

[57] L. Yang, D.R. Powell, R.P. Houser, Structural variation in copper(i) complexes with pyridylmethylamide ligands: structural analysis with a new four-coordinate geometry index, $\tau 4$, J. Chem. Soc. Dalt. Trans. (2007) 955–964, doi:10.1039/b617136b.

[58] F.H. Allen, The Cambridge Structural Database: a quarter of a million crystal structures and rising, Acta Crystallogr. Sect. B Struct. Sci. 58 (2002) 380–388, doi:10.1107/S0108768102003890.

[59] C. Foces-Foces, F.H. Cano, S. García-Blanco, Structure of bis[*dichloro*-*μ*-*bis*(3,5-*dimethyl*-4-*pyrazolyl*)*methane*-*cobalt*(II)]–ethanol (3:2), C22H32Cl4Co2N8.2/3C2H6O, Acta Crystallogr. Sect. C Cryst. Struct. Commun 39 (1983) 977–980, doi:10.1107/s0108270183007064.

[60] J. Lim, Y. Son, G. Gu, S. Ryu, D. Yoshioka, M. Mikuriya, Dinuclear Cobalt(II) complex with N,N,N′,N′-Tetrakis(3,5-dimethyl-1-pyrazolyl)methyl-1,4-phenylenediamine having a tetrahedral coordination geometry, X-ray struct, Anal. Online. 31 (2015) 25–26, doi:10.2116/xraystruct.31.25.

[61] A. Beheshti, F. Safaeiyan, F. Hashemi, H. Motamedi, P. Mayer, G. Bruno, H.A. Rudbari, Synthesis, structural characterization, antibacterial activity and computational studies of new cobalt (II) complexes with 1,1,3,3-tetrakis (3,5-dimethyl-1-pyrazolyl)propane ligand, J. Mol. Struct. 1123 (2016) 225–237, doi:10.1016/j.molstruc.2016.06.037.

[62] K.V. Domasevitch, Cobalt(II) chloride complexes with 1,1'-dimethyl-4,4'-bipyrazole featuring first- and second-sphere coordination of the ligand, Acta Crystallogr. Sect. C Struct. Chem. 70 (2014) 272–276, doi:10.1107/S2053229614002046.

[63] A.W. Addison, T.N. Rao, J. Reedijk, J. van Rijn, G.C. Verschoor, Synthesis, structure, and spectroscopic properties of copper(⟨scp⟩II⟨/scp⟩) compounds containing nitrogen–sulphur donor ligands; the crystal and molecular structure of aqua[1,7-*bis*(N-*methylbenzimidazol*-2′-*yl*)-2,6-*dithiaheptane*]copper(⟨scp⟩II⟨/scp⟩) pe, J. Chem. Soc., Dalt. Trans. (1984) 1349–1356, doi:10.1039/DT9840001349.

[64] L.R. Falvello, Jahn-Teller effects in solid-state co-ordination chemistry, J. Chem. Soc. - Dalt. Trans. (1997) 4463–4475, doi:10.1039/a703548i.

[65] P. Kapoor, A.P.S. Pannu, M. Sharma, M.S. Hundal, R. Kapoor, M. Corbella, N. Aliaga-Alcalde, Syntheses, X-ray crystal structure and magnetic studies of a new dinuclear CuII complex, [Cu2(*μ*-Cl)2L2Cl2]·2CH3CN, L: N,N,N′,N′-tetraisopropylpyridine-2,6-dicarboxamide, J. Mol. Struct. 981 (2010) 40–45, doi:10.1016/j.molstruc.2010.07.021.

[66] R.F. Semeniuc, D.L. Reger, Metal complexes of multitopic, third generation poly(pyrazolyl)methane ligands: multiple coordination arrangements, Eur. J. Inorg. Chem. 2016 (2016) 2253–2271, doi:10.1002/ejic.201600116.

[67] W.K. Chang, G.H. Lee, Y. Wang, T.I. Ho, Y.O. Su, Y.C. Lin, Synthesis, properties and molecular structure of copper(II) and cobalt(II) 1,2-bis(pyrazol-1-ylmethyl)benzene complexes, Inorganica Chim. Acta. 223 (1994) 139–144, doi:10.1016/0020-1693(94)03958-5.

[68] D.P. Pienaar, R.K. Mitra, T.I. va. Deventer, A.L. Botes, Synthesis of a variety of optically active hydroxylated heterocyclic compounds using epoxide hydrolase technology, Tetrahedron Lett. 49 (2008) 6752–6755, doi:10.1016/j.tetlet.2008.08.097.

[69] E.E. Benson, A.L. Rheingold, C.P. Kubiak, Synthesis and characterization of 6, 60-(2, 4, 6-triisopropylphenyl)-2, 20-bipyridine (tripbipy) and its complexes of the late first row transition metals, Inorg. Chem. 49 (2010) 1458–1464, doi:10.1021/ic9016382.

[70] V. Vrábel, L. Svorc, N. Juristová, J. Miklovič, J. Kozíšek, Bis(1-benzofuro[3,2-*c*]pyridine-kN)dichloridocobalt(II), Acta Crystallogr. Sect. E Struct. Reports Online. 63 (2007), doi:10.1107/S160053680704161X.

[71] H. Ohi, Y. Tachi, S. Itoh, Supramolecular and coordination polymer complexes supported by a tripodal tripyridine ligand containing a 1,3,5-triethylbenzene spacer, Inorg. Chem. 43 (2004) 4561–4563, doi:10.1021/ic049468j.

[72] Y. Xi, W. Wei, Y. Xu, X. Huang, F. Zhang, C. Hu, Coordination polymers based on substituted terpyridine ligands: synthesis, structural diversity, and highly efficient and selective catalytic oxidation of benzylic c-h bonds, Cryst. Growth Des. 15 (2015) 2695–2702, doi:10.1021/acs.cgd.5b00008.

[73] P. Grosshans, A. Jouaiti, V. Bulach, J.M. Planeix, M.W. Hosseini, N. Kyritsakas, Design and structural analysis of metallamacrocycles based on a combination

of ethylene glycol bearing pyridine units with zinc, cobalt and mercury, Eur. J. Inorg. Chem. 1 (2004) 453–458, doi:10.1002/ejic.200300598.
[74] C. Huang, Y. Wang, C. Wei, N. Li, F. Ji, J. Wu, H. Hou, Cation-exchange-induced single-crystal-to-single-crystal transformations of a nanoporous coordination complex, Inorg. Chem. Commun. 32 (2013) 68–73, doi:10.1016/j.inoche.2013.03.025.
[75] S. Sanz, H.M. O'Connor, V. Martí-Centelles, P. Comar, M.B. Pitak, S.J. Coles, G. Lorusso, E. Palacios, M. Evangelisti, A. Baldansuren, N.F. Chilton, H. Weihe, E.J.L. McInnes, P.J. Lusby, S. Piligkos, E.K. Brechin, [M2IIIM3II]n+ trigonal bipyramidal cages based on diamagnetic and paramagnetic metalloligands, Chem. Sci. 8 (2017) 5526–5535, doi:10.1039/c7sc00487g.
[76] F. Zhang, C.R.R. Adolf, N. Zigon, S. Ferlay, N. Kyritsakas, M.W. Hosseini, Molecular tectonics: hierarchical organization of heterobimetallic coordination networks into heterotrimetallic core-shell crystals, Chem. Commun. 53 (2017) 3587–3590, doi:10.1039/c7cc01455d.
[77] J. Dalbavie, J. Regnouf-de-vains, R. Lamartine, M. Perrin, S. Lecocq, B. Fenet, FULL PAPER A Calix [4]arene-based bipyridine podand as versatile ligand for, (2002).
[78] L. Álvarez-Miguel, I. Álvarez-Miguel, J.M. Martín-Álvarez, C.M. Álvarez, G. Rogez, R. García-Rodríguez, D. Miguel, Copper complexes for the promotion of iminopyridine ligands derived from β-alanine and self-aldol additions: relaxivity and cytotoxic properties, Dalt. Trans. 48 (2019) 17544–17555, doi:10.1039/C9DT03822A.
[79] Ł. Balewski, F. Sączewski, P. Bednarski, M. Gdaniec, E. Borys, A. Makowska, Structural diversity of copper(II) complexes with N-(2-pyridyl)imidazolidin-2-ones(Thiones) and their in vitro antitumor activity, Molecules 19 (2014) 17026–17051, doi:10.3390/molecules191017026.
[80] A.J. Blake, N.R. Brooks, N.R. Champness, P.A. Cooke, M. Crew, A.M. Deveson, L.R. Hanton, P. Hubberstey, D. Fenske, M. Schröder, Copper(I) iodide coordination networks–controlling the placement of (CuI)∞ ladders and chains within two-dimensional sheets, Cryst. Eng. 2 (1999) 181–195, doi:10.1016/S1463-0184(99)00018-0.
[81] A.N. Papadopoulos, V. Tangoulis, C.P. Raptopoulou, A. Terzis, D.P. Kessissoglou, First example of a CuII polymeric complex having a tetranuclear repeating unit with a S = 2 ground state. Crystal structure of [Cu4(dpk·CH3O)2Cl6] n (dpk·CH3OH = unimethylated diol of Di-2-pyridyl Ketone), Inorg. Chem. 35 (1996) 559–565, doi:10.1021/ic950659j.
[82] J. Juanhuix, F. Gil-Ortiz, G. Cuní, C. Colldelram, J. Nicolás, J. Lidón, E. Boter, C. Ruget, S. Ferrer, J. Benach, Developments in optics and performance at BL13-XALOC, the macromolecular crystallography beamline at the Alba Synchrotron, J. Synchrotron Radiat. 21 (2014) 679–689, doi:10.1107/S160057751400825X.
[83] Bruker APEX3 Software, (2019).
[84] G.M. Sheldrick, SHELXT – Integrated space-group and crystal-structure determination, Acta Crystallogr. Sect. A Found. Adv. 71 (2015) 3–8, doi:10.1107/S2053273314026370.
[85] G.M. Sheldrick, Crystal structure refinement with SHELXL, Acta Crystallogr. Sect. C Struct. Chem 71 (2015) 3–8, doi:10.1107/S2053229614024218.
[86] O.V. Dolomanov, L.J. Bourhis, R.J. Gildea, J.A.K. Howard, H. Puschmann, OLEX2: a complete structure solution, refinement and analysis program, J. Appl. Crystallogr. 42 (2009) 339–341, doi:10.1107/S0021889808042726.
[87] L. Krause, R. Herbst-Irmer, G.M. Sheldrick, D. Stalke, Comparison of silver and molybdenum microfocus X-ray sources for single-crystal structure determination, J. Appl. Crystallogr. 48 (2015) 3–10, doi:10.1107/S1600576714022985.
[88] C.F. Macrae, P.R. Edgington, P. McCabe, E. Pidcock, G.P. Shields, R. Taylor, M. Towler, J. van de Streek, Mercury : visualization and analysis of crystal structures, J. Appl. Crystallogr. 39 (2006) 453–457, doi:10.1107/S002188980600731X.
[89] C.F. Macrae, I.J. Bruno, J.A. Chisholm, P.R. Edgington, P. McCabe, E. Pidcock, L. Rodriguez-Monge, R. Taylor, J. van de Streek, P.A. Wood, Mercury CSD 2.0 – new features for the visualization and investigation of crystal structures, J. Appl. Crystallogr. 41 (2008) 466–470, doi:10.1107/S0021889807067908.
[90] C. Cason, T. Froehlich, C. Lipka, POV-Ray For Windows, Persistence of Vision Raytracer Pty, Persistence Vis, Pty. Ltd., Williamstown, Victoria, Aust, 2013 (Version 3.7).